



Research paper

Monte Carlo simulations of the fracture resistance degradation of asphalt concrete subjected to environmental factors

Cezary Szydłowski¹, Łukasz Smakosz²,
Marcin Stienss³, Jarosław Górski⁴

Abstract: The paper presents the results of laboratory tests of SCB (semi-circular beam) samples of asphalt concrete, subjected to the destructive effect of water and frost as well as the aging processes. The determined values of material parameters show significant dispersions, which makes the design of mixtures difficult. Statistical analysis of the test results supplemented by computer simulations made with the use of the proprietary FEM model was carried out. The main distinguishing feature of the model is the assignment of material parameters of coarse aggregate and bituminous mortar to randomly selected finite elements. The parameters of the mortar are selected by trial and error to match the numerical results to the experimental ones. The stiffness modulus of the bituminous mortar is, therefore, a substitute parameter, taking into account the influence of many factors, including material degradation resulting from the aging and changing environmental conditions, the influence of voids, and contact between the aggregate and the bituminous mortar. The use of the Monte Carlo method allows to reflect the scattering of the results obtained based on laboratory tests. The computational algorithm created in the ABAQUS was limited only to the analysis of the global mechanical bending response of the SCB sample, without mapping the failure process in detail. The combination of the results of laboratory tests usually carried out on a limited number of samples and numerical simulations provide a sufficiently large population of data to carry out a reliable statistical analysis, and to estimate the reliability of the material designed.

Keywords: asphalt concrete, numerical modeling, Monte Carlo method

¹MSc., Eng., Gdańsk University of Technology, Faculty of Civil and Environmental Engineering, Department of Highway and Transportation Engineering, 11/12 Gabriela Narutowicza Street, 80-233 Gdańsk, Poland, e-mail: cezary.szydowski@pg.edu.pl, ORCID: 0000-0002-6141-9839

²PhD., Eng., Gdańsk University of Technology, Faculty of Civil and Environmental Engineering, Department of Structural Mechanics, 11/12 Gabriela Narutowicza Street, 80-233 Gdańsk, Poland, e-mail: lukasz.smakosz@pg.edu.pl, ORCID: 0000-0003-3731-1681

³PhD., Eng., Gdańsk University of Technology, Faculty of Civil and Environmental Engineering, Department of Highway and Transportation Engineering, 11/12 Gabriela Narutowicza Street, 80-233 Gdańsk, Poland, e-mail: marcin.stienss@pg.edu.pl, ORCID: 0000-0003-1811-1086

⁴Prof., DSc., PhD., Eng., Gdańsk University of Technology, Faculty of Civil and Environmental Engineering, Department of Structural Mechanics, 11/12 Gabriela Narutowicza Street, 80-233 Gdańsk, Poland, e-mail: jaroslaw.gorski@pg.edu.pl, ORCID: 0000-0002-6478-0216

1. Introduction

Improving the quality of road construction is of great importance for driving safety while optimizing the costs of road infrastructure development. Designing asphalt mixtures is strictly related to laboratory research. Proper determination of the material parameters of mixtures based on the test results is difficult, as they are usually highly dispersed [1–4]. The mixture selection process should therefore be supplemented with probabilistic analyzes and reliability estimation.

Due to the structure of asphalt mixtures (heterogeneity of the material, including bituminous binders, mineral aggregate, and voids) and the scatter of test results, new methods of measurements carried out during laboratory tests are investigated, often directly related to advanced numerical analysis [5]. Precise mapping of the structure of mixtures could be achieved using digital image correlation [6] and X-ray Computed Tomography [7]. On this basis, homogenized models of material or the representative volume element (RVE) are built [8]. Random variables and random fields are also used in the description of asphalt mixtures [9]. The cracking of samples is simulated using cohesive elements [10, 11]. All analyzes are usually limited to a specific load or temperature range, as it is difficult to formulate general algorithms describing the mechanical behavior of bituminous material considering its viscoelastic nature.

The paper presents an analysis of the influence of environmental factors on the change of material parameters of asphalt mixtures [12, 13]. In order to assess the phenomenon, laboratory tests were carried out on SCB samples, taking into account the damaging effects of water and frost as well as the long-term aging processes of the mixtures. The influence of both factors occurring simultaneously was also verified. The analysis was limited to one type of asphalt concrete, tested at a selected temperature and loading rate.

The results of laboratory tests are characterized by dispersions, which should be included in the FEM material model. The proposed original material model [14] allows taking this feature into account in numerical simulations by using a random distribution of coarse aggregate and asphalt mortar. To simplify the FEM model, a substitute stiffness modulus of asphalt mortar E_{bit}^S was introduced, which captures the influence of many different factors, e.g. the effect of water and frost, material aging, contact between aggregate and mortar, as well as geometrical imperfections of samples and other, difficult to identify factors. The model does not accurately reflect the fracture process, but only the global characteristics of the mechanical behavior of SCB samples. The purpose of the calculations made with the ABAQUS software [15] is to increase the number of analyzed samples so that, in combination with laboratory tests, a reliable probabilistic analysis of the results can be performed. The proposed solutions can be used directly in assessing the reliability of asphalt mixtures.

2. Laboratory tests

Laboratory tests were carried out on asphalt concrete samples for the wearing course AC 11 S 50/70 KR3÷4 (medium traffic: from 0.5×10^6 to 7.3×10^6 of 100 kN standard axle loads) designed according to EN 13108-1. The composition of the mixture is presented in



Table 1. A volumetric distinction of asphalt concrete into a two-phase material model is also included. It consists of coarse aggregate and mortar (fine aggregate with filler, binder, and air voids) with volumes of 52.8% and 47.2%, respectively.

Table 1. Composition of asphalt concrete

Property	Composition [%]			
	Mineral mix, by mass	Mineral-asphalt mix, by mass	Mineral-asphalt mix, by volume	FEM two-phase material mix, by volume
Coarse aggregate 8/11 (granite)	25.0	23.6	20.9	52.8
Coarse aggregate 5/8 (granite)	15.0	14.2	12.6	
Coarse aggregate 2/5 (granite)	23.0	21.7	19.3	
Fine aggregate 0/2 (granite)	30.0	28.3	25.1	47.2
Limestone filler (limestone)	7.0	6.6	5.9	
Bitumen 50/70	–	5.6	14.0	
Voids	–	–	2.2	

Asphalt mixture was prepared using a laboratory mixer according to EN 12697-35 and subjected to short-term aging before specimen compaction according to the AASHTO R 30-2 procedure. Samples for SCB testing were prepared using a gyratory compactor with a diameter of 150 mm and a height of 105 mm. Four SCB samples were cut out from a single gyratory specimen. The process was set to achieve $7 \pm 0.5\%$ voids content in every SCB specimen.

The evaluation of changes in fracture toughness was carried out based on the results of testing SCB specimens with a 10 mm notch depth at a temperature of $+10^\circ\text{C}$, at a loading rate of 1 mm/min. A standard testing machine with a thermal chamber was used. The research scheme is shown in Fig. 1. The typical course of the $F - d$ relationship is shown in Fig. 2.

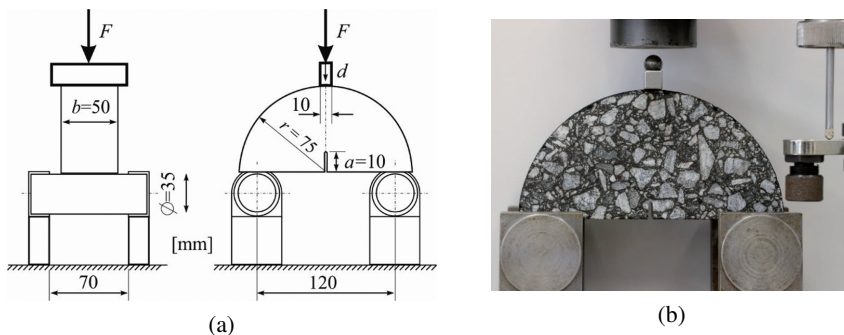


Fig. 1. The scheme of semi-circular bending test (a) and view of the test sample (b)



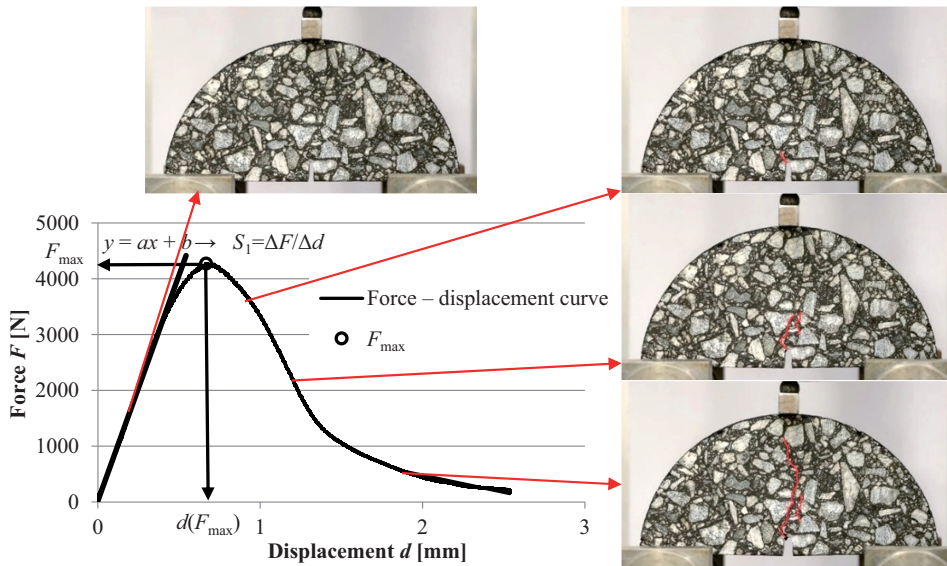


Fig. 2. A typical shape of the force-displacement curve with the sample's fracture scheme

Due to the different methods of assessing resistance to water and frost, the tests were carried out according to several selected variants of conditioning the samples presented in Table 2. In each case, four SCB samples were tested. The assessment of the influence of aging of the mixtures on the fracture toughness was made based on long-term conditioning according to AASHTO R 30-02. The conditioning involves keeping samples in an airflow fan at the temperature of 85°C for 120 hours. The test simulates a ten-year service life of the pavement. Additionally, an extended long-term aging simulation process of 216 hours was carried out, which simulates approximately twenty years of pavement operation [16, 17]. In order to evaluate the simultaneous influence of both factors, some samples subjected to the influence of water and frost were conditioned after long-term aging. A total of 10 variants were tested (Table 3).

A group of 40 results was obtained, taking into account both the dispersion due to material heterogeneity (four samples for each of the conditioning variants) and variation in material properties caused by environmental factors (10 conditioning variants). Since all the tested samples were prepared and compacted in the same way, it can be assumed that the material constructed into pavement has the same parameters as unconditioned samples. The remaining results represent the parameters of the material that has been subjected to varying environmental influences during its service life. Thus, the obtained group of results can be regarded as parameters of material in varying degrees of environmental degradation, corresponding to the pavement after a twenty-year operational period. The obtained $F - d$ relationships are shown in Fig. 3. Based on the results obtained, it can be concluded that the interaction of water and frost action caused a decrease in maximum force and thus a decrease in fracture toughness. Long-term aging stiffened the asphalt binder.

Table 2. Summary of water and frost conditioning schemes

Conditioning stage	Conditions according to the procedure			
	WT:2-2010	WT:2-2014	AASHTO T 283	AASHTO TP 140 (MiST)
Saturation of samples with water	Vacuum chamber; 20 ± 5°C; pressure 6.7 ± 0.3 kPa	Vacuum chamber; 20 ± 5°C; pressure 6.7 ± 0.3 kPa; required degree of saturation 55÷80%	Vacuum chamber; pressure 13÷67 kPa; required degree of saturation 70÷80%	Lack of step
The action of water at increased temperature	Water bath; 40 ± 1°C; 68÷72 hours	Water bath; 40 ± 1°C; 68÷72 hours	Lack of step	Device chamber; 60 ± 1°C; 20 hours; next 3 500 cycles of pressure changes to 40 PSI at 60 ± 1°C
Freezing	Freezer; -18 ± 3°C; minimum 16 hours	Freezer; -18 ± 3°C; minimum 16 hours	Freezer; -18 ± 3°C; minimum 16 hours	Lack of step
Thawing	Water bath; 60 ± 1°C; 24 ± 1 hours	Water bath; 25 ± 2°C; 24 ± 1 hours	Water bath; 60 ± 1°C; 24 ± 1 hours	Lack of step
Conditioning prior to testing	Water bath; 25 ± 2°C; minimum 2 hours	Water bath; 25 ± 2°C; minimum 4 hours	Water bath; 25 ± 0.5°C; 2 hours ±10 minutes	Water bath; 25 ± 1.5°C; minimum 2 hours

Table 3. Summary of tested variants of conditioning of samples exposed to environmental factors

Conditioning of samples	STOA	LTOA 120h	LTOA 216h
No conditioning	x	x	x
WT:2-2010	x		
WT:2-2014	x	X	
AASHTO T 283	x	x	
AASHTO TP 140 (MiST)	x	x	

STAO – short-term oven aging, LTOA – long-term oven aging



There is a visible increase in the force at fracture F_{\max} and a decrease in the corresponding displacement $d(F_{\max})$. The combined effects of water, frost, and aging resulted in changes in the material leading to an increase the fracture toughness, but a reduction in displacement at fracture is visible.

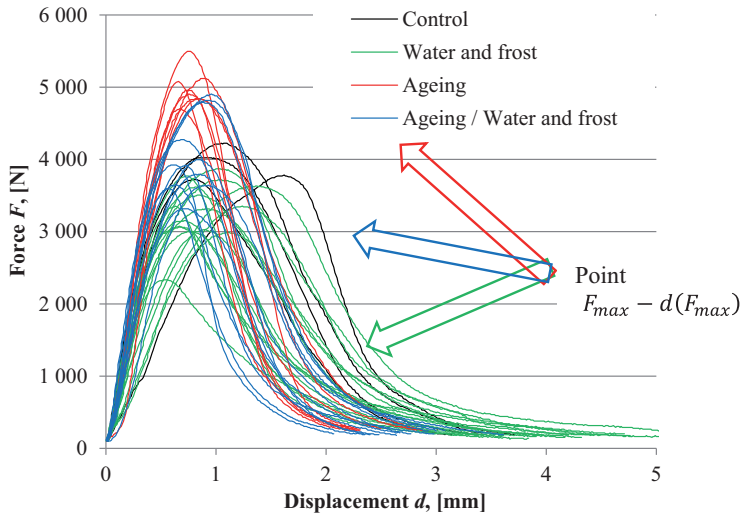


Fig. 3. Laboratory results of all the SCB bending tests performed

3. Numerical simulations

Laboratory tests (Fig. 3) can be extended by numerical analysis. The obtained solutions will increase the sample population and make it possible to conduct a probabilistic analysis. The FEM model should simulate the results of laboratory tests carried out on SCB samples, especially the load-displacement ($F - d$) diagrams. Due to the random nature of the results, the model should also reflect the dispersion of parameters such as initial (linear) stiffness of the sample (parameter S), maximum force F_{\max} , displacement $d(F_{\max})$, corresponding to this force, or the stress intensity factor K_{Ic} . However, it is not necessary to map the fracture processes of SCB samples in detail. Moreover, it was assumed that the proposed algorithm should represent one selected group of asphalt mix and the conditions of one test (temperature and deformation rate).

The proposed material model [14] assigns random parameters of coarse aggregate and asphalt mortar to finite elements, creating a substitute material structure, presented in Fig. 4.

The calculation algorithm is carried out in several steps. In the first stage, the method of generating the SCB sample model is selected. This process is related to the correlation between the aggregate size and the dimensions of finite elements. The algorithms proposed in [14] enable direct drawing of elements and combining them into a configuration



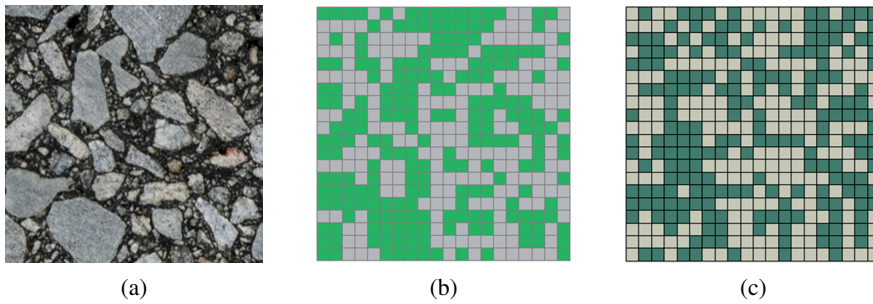


Fig. 4. Generation of a two-phase FEM material model: (a) – the actual fragment of the asphalt concrete sample, (b) – manual division into two phases, (c) – an example of the generated asphalt concrete structure using the uniform distribution of aggregate and asphalt mortar

corresponding to aggregate size and distribution. In the analyzed case, it was proposed to divide the medium into elements corresponding to the smallest grains of coarse aggregate (Table 1) – approximately 2 mm (Fig. 4). Based on the analysis of the mixture composition (Table 1), the FEM material model was defined as two-phase, i.e. 50% of the elements were randomly assigned the parameters of coarse aggregate, and the remaining elements were assigned the parameters of asphalt mortar (Fig. 5). The model does not take into account air voids as a separate material because the introduction of an additional, third phase would require the adoption of a different, uneven finite element division. For the same reason, mesh density in the fracture-initiating notch area was not increased. It causes no difficulties since the failure process is mapped by cohesive elements located in the axis of symmetry of the SCB sample (Fig. 5). Such simplification of the analysis seems sufficient in this case.

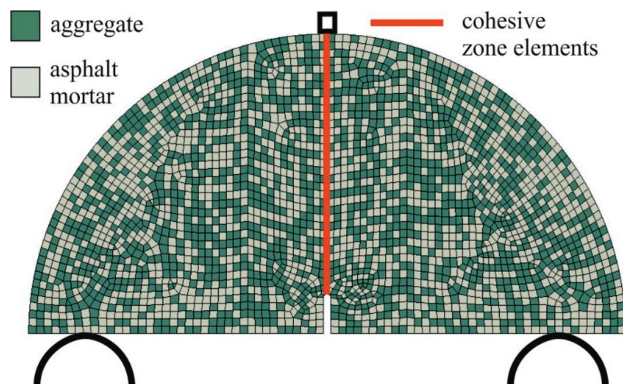


Fig. 5. Two-phase FEM model of the SCB sample obtained by the randomly generated elements

In the second step, the material parameters reflecting the initial linear-elastic behavior of the SCB sample were selected (Figs. 2 and 3). The following aggregate parameters were adopted: $E_{agg} = 60\,000$ MPa and $\nu_{agg} = 0.2$ [18]. It was assumed that the material

data of the aggregate did not change even in the case of long-term environmental impact. The parameters of the asphalt mortar E_{bit} were selected by trial and error in such a way as to fit the initial linear $F - d$ relationship obtained from numerical calculations to the results of laboratory tests (Fig. 3). Although these parameters can be determined directly in the laboratory [14, 19], their substituted values E_{bit}^S are introduced in the model, unrelated to the actual E_{bit} values. This way, the interpretation of the parameter E_{bit}^S was extended. It includes several factors influencing the numerical solution, i.e. the simulation of the material degradation process resulting from the aging and changing environmental conditions, the influence of voids or contact between the aggregate and the bituminous mortar. It is therefore necessary to link the initial stiffness of the sample determined by the S parameter (Fig. 2) with the numerical solution. As several different groups of samples are analyzed simultaneously, a wide result range was adopted, in which S varies from 4000 to 13 000 (Fig. 6). In order to simplify the calculations, the relationship between S and F_{max} was approximated linearly (Fig. 6):

$$(3.1) \quad F_{\text{max}}^S = 0.2269S + 2015.7, \quad S \in (4000, 13\,000)$$

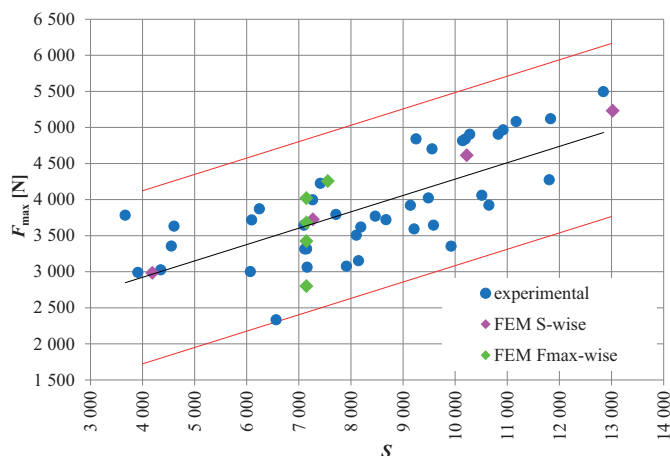


Fig. 6. Experimental results; force F_{max} as a function of sample stiffness S ; the pink (magenta) color marks the results of numerical calculations estimating the values $E_{\text{bit}}^S = E_{\text{bit}}^S(S)$; the results that estimate the values $F_{\text{max}}^S = F_{\text{max}}^S(S)$ are marked green

The equivalent value of the mortar stiffness modulus E_{bit}^S was determined by trial and error: for $S = 4000 \rightarrow E_{\text{bit}}^{4000} = 80$ MPa and for $S = 13\,000 \rightarrow E_{\text{bit}}^{13\,000} = 300$ MPa. It is assumed that the change of the equivalent stiffness modulus between these values is linear:

$$(3.2) \quad E_{\text{bit}}^S = 0.0244S - 17.778, \quad S \in (4000, 13\,000)$$

Using the equation (3.1), this formula can also be written in the F_{max}^S function:

$$(3.3) \quad E_{\text{bit}}^S = 0.1077F_{\text{max}}^S - 234.89, \quad F_{\text{max}}^S \in (3000, 5000), \quad S \in (4000, 13\,000)$$



In the third step of the analysis, the parameters initiating the fracture of the sample are selected, and thus, most of all, determining the value of the maximum force F_{\max} obtained during the test (Figs. 3 and 6). The course of cracking and weakening of the material is described only by the parameters of the cohesive elements connecting both fragments of the SCB sample (Fig. 5). The parameters of the cohesive connection (Fig. 7) are determined numerically by trial and error. The maximum breaking stress σ_f is selected to relate it to the laboratory results: for $S = 4000 \rightarrow F_{\max}^{4000} = 2930 \text{ N} \rightarrow \sigma_f^{4000} = 1.3 \text{ MPa}$ and for $S = 13000 \rightarrow F_{\max}^{13000} = 4960 \text{ N} \rightarrow \sigma_f^{13000} = 1.8 \text{ MPa}$. The limit stresses between these extreme values are approximated linearly (Fig. 6):

$$(3.4) \quad \sigma_f^S = 0.0002F_{\max}^c + 0.5783, \quad F_{\max}^S \in (3000, 5000), S \in (4000, 13000)$$

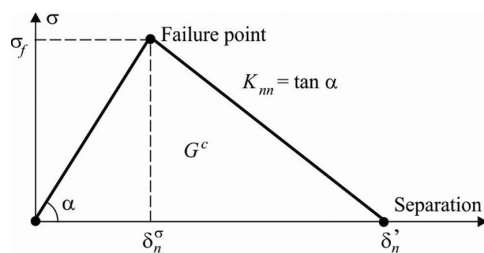


Fig. 7. Cohesive contact linear damage evolution model [Abaqus]

The last, fourth step of the calculation algorithm is the adoption of the maximum force distribution F_{\max} related to the initial stiffness of the sample S (Fig. 3). In accordance with the results presented in Fig. 6, it was assumed that the change in the F_{\max} value is located around the average value approximated by a straight line ($S - F_{\max}$). Assuming that the distribution of F_{\max} can be described by a normal distribution, an envelope $\pm 3\sigma_{F_{\max}} = 1200 \text{ N}$ was introduced. The values of $\sigma_f^{S, F_{\max}}$ parameters in this range were determined by the trial and error method based on the laboratory test results of a selected group of five samples for which $S \cong 7000$ (Fig. 6). The obtained parameters are shown in Fig. 8. The relationship between F_{\max} and $\sigma_f^{S, F_{\max}}$ is linear:

$$(3.5) \quad \sigma_f^{7000, F_{\max}} = 0.0005F_{\max}^{7000} - 0.4 \text{ [MPa]}, \quad F_{\max}^{7000} \in (3000, 4200)$$

In the case of other values of S in the range of $S = 3000 \div 13000$, they are assumed as follows:

$$(3.6) \quad \sigma_f^S = 0.0005F_{\max}^S - 0.4 \text{ [MPa]}$$

The parameter G_c related to the weakening (Fig. 7) was selected as equal in σ_f^S value. This approach allowed for obtaining curves with proportions similar to the experimental results. It should be emphasized that all calculations were performed for the same randomly selected SCB sample model. Thus, the only variable was the substitute mortar modulus

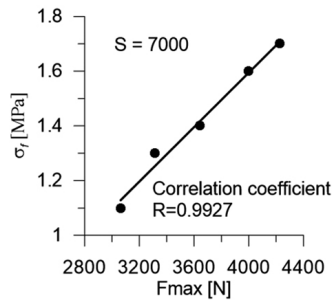


Fig. 8. Numerical adjustment of σ_f^S values, taking into account the dispersions around the mean values: five $F - d$ plots and the corresponding values σ_f^S , linear relationship $\sigma_f^S - F_{\max}$

E_{bit}^S , and the variable value of the failure parameter σ_f^S , the distribution of aggregate in the sample did not change.

After performing the preliminary calculations, the course of calculations of the $F - d$ plot for a sample from any range $S = 3000 \div 13\,000$ is as follows:

- 1) selection or randomization of parameter S from the uniform distribution $S = 3000 \div 13\,000$,
- 2) F_{\max}^S determination based on the randomly selected S parameter (Eq. (3.1)),
- 3) determination of the parameter E_{bit}^S based on the linear approximation of the results in the range $E_{\text{bit}}^{4000} \div E_{\text{bit}}^{13\,000}$ (Eq. (3.2) or (3.3)),
- 4) randomization of the dispersion parameter around the mean F_{\max}^S of the normal distribution $F_{\max}^S \pm 3\sigma_{F_{\max}^S}$,
- 5) determining the parameter $\sigma_f^{S, F_{\max}}$ according to Eq. (3.6).

The created proprietary algorithms allow to perform calculations from any range of laboratory tests. Exemplary calculations were performed for 27 cases, they are presented in Fig. 9. All the results are within the range obtained based on laboratory tests.

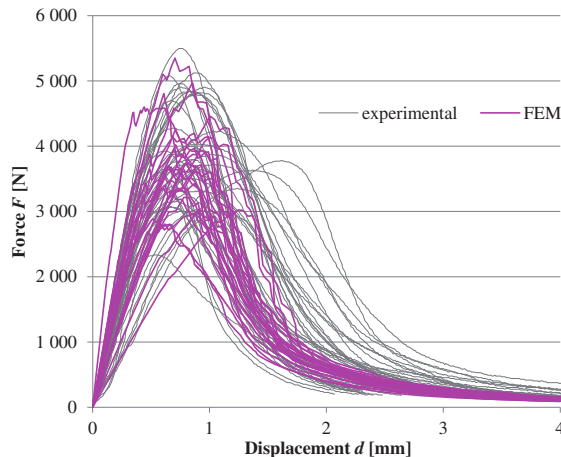


Fig. 9. Results of numerical calculations



4. Conclusions

Comprehensive tests of SCB samples subjected to environmental factors simulating the road degradation process during its service life as well as numerical calculations supplementing the results of laboratory tests allow for the formulation of the following conclusions:

1. The results of laboratory tests taking into account the influence of water and frost action on the mechanical response of the tested samples showed significant dispersions of basic material parameters related mainly to the time-lapse during service life. Not only deterministic (expected) values of these parameters are changed, but also the uncertainty of their determination (standard deviations).
2. Asphalt mix design algorithms should take into account material degradation over time.
3. The proprietary material model using the random distribution of coarse aggregate in the sample allows for the numerical simulation of laboratory tests, taking into account the change in the mechanical properties of the material under the influence of environmental factors. The introduced substitute parameter of asphalt mortar stiffness enables relatively easy consideration of the influence of all possible factors on the degradation of asphalt concrete parameters.
4. The presented calculation model has been calibrated for one investigated asphalt concrete, selected temperature, and loading rate. If the tested material or test conditions are changed, the calculation algorithm should be recalibrated.
5. The combination of laboratory test results with numerical analysis supplementing the sample population allows for probabilistic analysis and even reliability estimation related to the assessment of the durability of asphalt mixtures.

Acknowledgements

The authors acknowledge the access to computational software provided by the Centre of Informatics – Tricity Academic Supercomputer & network (CI TASK).

References

- [1] G. Nsengiyumva, T. You, and Y.-R. Kim, “Experimental-Statistical Investigation of Testing Variables of a Semicircular Bending (SCB) Fracture Test Repeatability for Bituminous Mixtures”, *Journal of Testing and Evaluation*, vol. 45, no. 5, art. no. 20160103, 2017, DOI: [10.1520/JTE20160103](https://doi.org/10.1520/JTE20160103).
- [2] N. Bala and M. Napiah, “Fatigue life and rutting performance modelling of nanosilica/polymer composite modified asphalt mixtures using Weibull distribution”, *International Journal of Pavement Engineering*, vol. 21, no. 4, pp. 497–506, 2020, DOI: [10.1080/10298436.2018.1492132](https://doi.org/10.1080/10298436.2018.1492132).
- [3] P. Singh and A.K. Swamy, “Probabilistic approach to characterise laboratory rutting behaviour of asphalt concrete mixtures”, *International Journal of Pavement Engineering*, vol. 21, no. 3, pp. 384–396, 2020, DOI: [10.1080/10298436.2018.1480780](https://doi.org/10.1080/10298436.2018.1480780).
- [4] P.J. Haghighat Pour, M.R.M. Aliha, and M. R. Keymanesh, “Evaluating mode I fracture resistance in asphalt mixtures using edge notched disc bend ENDB specimen with different geometrical and environmental conditions”, *Engineering Fracture Mechanics*, vol. 190, pp. 245–258, 2018, DOI: [10.1016/j.engfracmech.2017.11.007](https://doi.org/10.1016/j.engfracmech.2017.11.007).



- [5] H.R. Radeef, et al., “Linear viscoelastic response of semi-circular asphalt sample based on digital image correlation and XFEM”, *Measurement*, vol. 192, art. no. 110866, 2022, DOI: [10.1016/j.measurement.2022.110866](https://doi.org/10.1016/j.measurement.2022.110866).
- [6] B. Doll, H. Ozer, J. Rivera-Perez, I.L. Al-Qadi, and J. Lambros, “Damage zone development in heterogeneous asphalt concrete”, *Engineering Fracture Mechanics*, vol. 182, pp. 356–371, 2017, DOI: [10.1016/j.engfracmech.2017.06.002](https://doi.org/10.1016/j.engfracmech.2017.06.002).
- [7] Y. Huang, D. Yan, Z. Yang, and G. Liu, “2D and 3D homogenization and fracture analysis of concrete based on in-situ X-ray Computed Tomography images and Monte Carlo simulations”, *Engineering Fracture Mechanics*, vol. 163, pp. 37–54, 2016, DOI: [10.1016/j.engfracmech.2016.06.018](https://doi.org/10.1016/j.engfracmech.2016.06.018).
- [8] J. Wimmer, B. Stier, J.-W. Simon, and S. Reese, “Computational homogenisation from a 3D finite element model of asphalt concrete—linear elastic computations”, *Finite Elements in Analysis and Design*, vol. 110, pp. 43–57, 2016, DOI: [10.1016/j.finel.2015.10.005](https://doi.org/10.1016/j.finel.2015.10.005).
- [9] H. Li, Z. Yang, B. Li, and J. Wu, “A phase-field regularized cohesive zone model for quasi-brittle materials with spatially varying fracture properties”, *Engineering Fracture Mechanics*, vol. 256, art. no. 107977, 2021, DOI: [10.1016/j.engfracmech.2021.107977](https://doi.org/10.1016/j.engfracmech.2021.107977).
- [10] S. M. Motevalzadeh and H. Rooholamini, “Cohesive zone modeling of EAF slag-included asphalt mixtures in fracture modes I and II”, *Theoretical and Applied Fracture Mechanics*, vol. 112, art. no. 102918, 2021, DOI: [10.1016/j.tafmec.2021.102918](https://doi.org/10.1016/j.tafmec.2021.102918).
- [11] J. Kollmann, et al., “Parameter optimisation of a 2D finite element model to investigate the microstructural fracture behaviour of asphalt mixtures”, *Theoretical and Applied Fracture Mechanics*, vol. 103, art. no. 102319, 2019, DOI: [10.1016/j.tafmec.2019.102319](https://doi.org/10.1016/j.tafmec.2019.102319).
- [12] M.O. Hamzah, B. Golchin, and J. Voskuilen, “The combined effects of aging and moisture conditioning on the indirect tensile strength, flow and fracture energy of warm mix asphalt”, in *Bituminous Mixtures and Pavements VI*, A. Nikolaidis, Ed. London: Taylor & Francis Group, 2015, pp. 255–264, DOI: [10.1201/b18538-38](https://doi.org/10.1201/b18538-38).
- [13] P.K. Das, Y. Tasdemir, and B. Birgisson, “Evaluation of fracture and moisture damage performance of wax modified asphalt mixtures”, *Road Materials and Pavement Design*, vol. 13, no. 1, pp. 142–155, 2012, DOI: [10.1080/14680629.2011.644120](https://doi.org/10.1080/14680629.2011.644120).
- [14] C. Szydłowski, Ł. Smakosz, M. Stienss, and J. Górski, “The use of a two-phase Monte Carlo material model to reflect the dispersion of asphalt concrete fracture parameters”, *Theoretical and Applied Fracture Mechanics*, vol. 119, art. no. 103326, 2022, DOI: [10.1016/j.tafmec.2022.103326](https://doi.org/10.1016/j.tafmec.2022.103326).
- [15] M. Smith, *ABAQUS/Standard User's Manual, Version 6.9*. Providence, RI: Dassault Systèmes Simulia Corp, 2009.
- [16] C.A. Bell, A.J. Wieder, and M.J. Fellin, “Laboratory Aging of Asphalt-Aggregate Mixtures: Field Validation”, Strategic Highway Research Program A-390, National Research Council, Washington, DC, 1994.
- [17] S. Amani, A. Kavussi, and M. M. Karimi, “Effects of aging level on induced heating-healing properties of asphalt mixes”, *Construction and Buildings Materials*, vol. 263, art. no. 120105, 2020, DOI: [10.1016/j.conbuildmat.2020.120105](https://doi.org/10.1016/j.conbuildmat.2020.120105).
- [18] M.C. Villeneuve, et al., “Estimating in situ rock mass strength and elastic modulus of granite from the Soultz-sous-Forêts geothermal reservoir (France)”, *Geothermal Energy*, vol. 6, no. 1, art. no. 11, 2018, DOI: [10.1186/s40517-018-0096-1](https://doi.org/10.1186/s40517-018-0096-1).
- [19] G. Mazurek, “Effect of filler type on non-linear viscoelastic characteristics of asphalt mastic”, *Archives of Civil Engineering*, vol. 67, no. 2, pp. 247–259, 2021, DOI: [10.24425/ace.2021.137166](https://doi.org/10.24425/ace.2021.137166).



Symulacje Monte Carlo degradacji odporności na pęknięcie betonu asfaltowego pod wpływem czynników środowiskowych

Słowa kluczowe: beton asfaltowy, modelowanie numeryczne, metoda Monte Carlo

Streszczenie:

Oddziaływanie czynników środowiskowych zmienia parametry mieszanek mineralno-asfaltowych mających wpływ na odporność na pęknięcie. W celu oceny zjawiska wykonano badania laboratoryjne z uwzględnieniem niszczącego oddziaływania wody i mrozu oraz procesów starzenia eksploatacyjnego mieszanek. Weryfikacji poddano również wpływ obu czynników występujących jednocześnie.

Wyniki badań laboratoryjnych charakteryzują się rozrzutami. Zmienność cech powinna być uwzględniona w modelu materiałowym. Zaproponowany autorski model materiałowy pozwala uwzględnić tę cechę w symulacjach numerycznych poprzez wykorzystanie losowego rozkładu kruszywa grubego oraz zaprawy asfaltowej.

Na podstawie otrzymanych wyników laboratoryjnych stworzono algorytm losowo zmieniający parametry materiałowe zaprawy asfaltowej. W rezultacie umożliwiło to uzyskanie rozwiązań numerycznych uwzględniających jednocześnie rozrzuty wyników spowodowane niejednorodnością materiału oraz degradacją betonu asfaltowego pod wpływem oddziaływania czynników środowiskowych.

Z uwagi na różne metody oceny odporności na oddziaływanie wody i mrozu badania przeprowadzono według kilku wybranych wariantów kondycjonowania próbek. Oceny wpływu starzenia mieszanek na odporność na pęknięcie dokonano na podstawie metody AASHTO R 30-02. Dla oceny jednoczesnego wpływu obu czynników część próbek poddano starzeniu długoterminowemu przed symulacją oddziaływania wody i mrozu.

Badania zostały przeprowadzone na próbkach betonu asfaltowego do warstwy ścieralnej AC 11 S 50/70 KR3÷4. Ocenę zmian odporności na pęknięcie przeprowadzono na podstawie badania próbek SCB z nacięciem 10 mm w temperaturze +10°C, przy prędkości deformacji 1 mm/min.

Biorąc pod uwagę fakt, że wszystkie próbki poddane badaniom zostały przygotowane i zagęszczone w ten sam sposób, można przyjąć, że w momencie wbudowania w nawierzchnię materiał charakteryzuje się parametrami otrzymanymi jak dla próbek nie poddanych kondycjonowaniu. Pozostałe wyniki reprezentują parametry materiału, który został poddany naturalnemu oddziaływaniu czynników środowiskowych podczas eksploatacji nawierzchni. Otrzymaną grupę wyników można więc traktować jako parametry charakteryzujące materiał w różnym stopniu zmieniony pod wpływem czynników środowiskowych, a otrzymane parametry odwzorowują możliwe do uzyskania wartości w przypadku materiału pobranego z nawierzchni po różnym czasie eksploatacji.

Zaproponowany model materiałowy przyporządkowuje losowo parametry kruszywa grubego i zaprawy asfaltowej elementom skończonym tworząc zastępczą strukturę materiału. W celu symulacji degradacji cech materiałowych spowodowanych oddziaływaniem wody i mrozu oraz starzeniem eksploatacyjnym parametry mechaniczne zaprawy asfaltowej przyjmowane są także w sposób losowy.

Wyniki symulacji numerycznych w znacznym stopniu odpowiadają результатам badań doświadczalnych. Autorski model materiałowy wykorzystujący losowy rozkład kruszywa grubego w próbce pozwala na numeryczną symulację testów laboratoryjnych z uwzględnieniem zmiany cech mechanicznych materiału pod wpływem oddziaływania czynników środowiskowych. Wprowadzony zastępczy parametr sztywności zaprawy asfaltowej umożliwia stosunkowo łatwe uwzględnienie wpływu wszystkich możliwych czynników na degradację tych parametrów. Przedstawiony model obliczeniowy nie ma charakteru ogólnego. W przypadku zmiany testowanego materiału lub warunków wykonywania prób należy na nowo skalibrować algorytm obliczeniowy.

Received: 2022-07-04, Revised: 2022-08-05

